

# Multi-Objective Optimization Design of Permanent Magnet Spherical Motor based on PSO-BP Neural Network

Xiwen Guo<sup>1,2,3</sup>, Ronglin Zhang<sup>1,2</sup>, Qunjing Wang<sup>1,2,3</sup>, Yan Wen<sup>1,2</sup>, Nengwei Gong<sup>1,2</sup>

<sup>1</sup>School of Electrical Engineering and Automation, Anhui University, Hefei, Anhui, China

<sup>2</sup>National Engineering Laboratory of Energy-saving Motor & Control Technique, Anhui University, Hefei, Anhui, China

<sup>3</sup>Engineering Research Centre of Power Quality, Ministry of Education, Anhui University, Hefei, Anhui, China

## Abstract

Aimed at the problems of low output torque of permanent magnet spherical motor (PMSM), an effective multi-objective optimization design method to improve torque characteristics and reduce limited material volume, improve the motor load characteristics, reduce design costs is present. At first, based on finite element analysis (FEA) data, a particle swarm optimization-optimized BP neural network (PSO-BP) modelling method is proposed, which solves the modelling by drawing the nonlinear and complex relationship between structural parameters and torque problem. Then, an adaptive grid multi-objective particle swarm optimization (AGA-MOPSO) algorithm is proposed to search for the best structural parameters, and a Pareto optimization frontier map are obtained. Finally, according to the FEA simulation analysis, the best solution is selected from the Pareto optimization results. The simulation results show that compared with the original motor, the torque has increased by approximately 43.52% and the volume has decreased by approximately 7.8%, which proves the correctness and feasibility of this method.

**Keywords:** permanent magnet spherical motor (PMSM), multi-objective design optimization, finite element analysis (FEA), particle swarm optimization-optimized BP (PSO-BP), adaptive grid multi-objective particle swarm optimization algorithm (AGA-MOPSO)

*Received:* 10 January 2020

## To cite this article:

Xiwen Guo, Ronglin Zhang, Qunjing Wang, Yan Wen, Nengwei Gong, "Multi-objective optimization design of permanent magnet spherical motor based on PSO-BP neural network", in *Electrotehnica, Electronica, Automatica (EEA)*, 2019, vol. 67, no. 2, pp. 23-31, ISSN 1582-5175.

## 1. Introduction

The traditional multi-degree-of-freedom device is a combination of multiple single-degree-of-freedom motors and complex mechanical structures. The complex spatial motion is composed of single degree of freedom motors, which has many problems. For example, large volume, low system stiffness, poor control accuracy large volume, and poor control accuracy. In the actual use process, in order to improve the performance of the motor, we have to try to improve these deficiencies, and then the permanent magnet spherical motor appears. PMSM has the advantages of small size, light weight and high accuracy, and can be a good substitute for multi-degree-of-freedom devices. It has broad application prospects in high-tech fields such as aerospace, robotic arms and bionic vision [1], [2]. The optimal design of PMSM is a complex multi-objective, non-linear process [3]-[6]. In the optimization process, many design factors must be considered, design details are continuously improved, and evaluation and correction are repeated to obtain the best design solution. Among them, the relationship between the optimization goal and the structural parameters is the basis of the optimization design. In order to optimize the design of the motor, many methods have been used to establish the relationship

between the optimization objectives and the structural parameters, among which the analysis method and the finite element method are the best. In [7], a novel spherical force sensing system was proposed. The equivalent current method and the ampere force law are used to obtain the ampere torque. Based on the air gap magnetic flux density, the cogging torque was obtained by the Maxwell stress method. Finally, the adaptive particle swarm algorithm is used to optimize the structural parameters. The analytical method clearly expresses the relationship between the input parameters and the optimization goal, but the process is too tedious. In [8], the equivalent magnetic circuit method based on Maxwell tensor was used to analyse the electromagnetic torque of PMSM, and then the multi-objective immune algorithm was used to optimize the coil structure. When the structural parameters of PMSM are changed, the analysis results need to be recalculated, which will complicate the calculation process. The FEA finite element method optimizes the structural parameters by calculating the data multiple times and comparing the data, which requires a lot of time [9]. In order to improve the efficiency of the FEA method, a polynomial-based RSM was proposed in [10] to optimize the torque of a multi-degree-of-freedom permanent magnet spherical motor, and a finite element analysis method was used to establish a

numerical model of the response surface equation. With the increase of samples, the approximation accuracy has not been effectively improved, and when the dimension and polynomial order of the design variables increase, the calculation amount will also increase rapidly. In [11], [12], the support vector machine (SVM) method was used to draw the relationship between the structural parameters and torque of the permanent magnet spherical motor. In fact, the SVM method is suitable for the situation where the training sample data space is small, and there are certain limitations in the optimization design for multiple parameters.

In recent years, intelligent algorithms have been widely used in many fields [13]-[24]. The emergence and wide application of intelligent algorithms bring great convenience to data processing. Each algorithm has its advantages and disadvantages, which requires users to understand the principle of the algorithm and use the most appropriate and accurate algorithm to achieve the research purpose. In these algorithms, the PSO-BP neural network method and AGA-MOPSO algorithm have the advantages of simple modelling process, moderate calculation amount, high efficiency, and good accuracy. Therefore, in view of the problems existing in the above methods, this paper focuses on the optimization design method combining PSO-BP neural network method [25]-[27] and AGA-MOPSO algorithm [28]. Firstly, the electromagnetic torque of a single pole and a single coil of permanent magnet is obtained by finite element analysis. On this basis, the PSO-BP neural network method is used to establish the torque model, and the electromagnetic torque under different combinations of structural factors is obtained through factorial design. Through the FEA method to obtain the sample data, and then through the iterative operation, the relationship between the structure and the electromagnetic torque can be accurately predicted. Then AGA-MOPSO algorithm is used to optimize the structural parameters. Finally, the FEA analysis method is used to compare the initial PMSM structural parameters with the optimized PMSM structural parameters. Simulation results verify the accuracy and effectiveness of the method.

## 2. Torque analysis of PMSM

The torque analysis of PMSM is the key to the optimization of the spherical motor structure. The acquisition of torque is the prerequisite for all optimization work. When the structural parameters of the motor change, the torque output will also change. Only by obtaining the accurate torque value under a certain structure can accurate structural optimization be performed. The commonly used methods are the superposition principle and the finite element method.

### 2.1 The basic structure of PMSM

PMSM is composed of an output shaft, a spherical rotor and a stator. The structure of PMSM has been described in [29], The stator coil is electrified according to a certain electrifying strategy, and the current will be affected by the magnetic field force, so that the spherical rotor and the output shaft move. The specific structure is as follows: 40 permanent

magnets are evenly embedded on the rotor ball surface according to the principle of alternating N and S poles. 40 permanent magnets are divided into 4 layers, each layer has 10 permanent magnets, and the interval between the two layers is  $30^\circ$ . The 24 stator coils are divided into two layers, which are arranged evenly on the stator shell. The interval between the two layers of stator coils is  $44^\circ$ . The spherical rotor is made of stainless steel, the permanent magnet is made of NdFe35, and the stator coil is of hollow cylindrical structure. Load is installed on the output shaft, and the motor drives the load to complete the target movement.

The prototype of PMSM is shown in Figure 1.

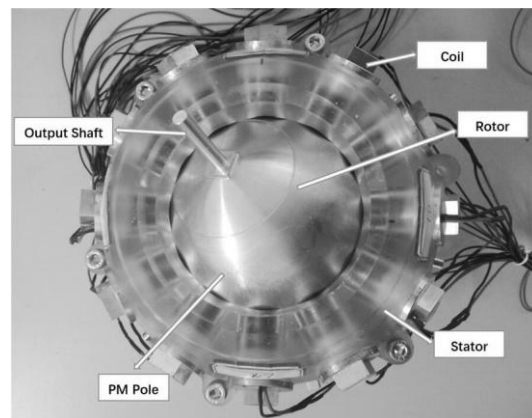


Figure 1. Structure diagram of PMSM

The detailed parameters of PMSM are introduced in detail here. The radius of rotor  $r_1$  is 65 mm. The length of PM pole  $h_1$  is 12 mm. The radius of PM pole  $r_2$  is 10mm. The relative permeability of PM pole  $\mu$  is 1.099. The NI is 1200. The inner radius of coil  $r_3$  is 4 mm. The outer radius of coil  $r_4$  is 14 mm. The height of coil  $h_2$  is 25 mm. These parameters are the original parameters of the motor in this paper. Obviously, when the structural parameters change, the performance of the motor will inevitably change.

### 2.2 Torque analysis

Since there are not ferromagnetic materials in the PM poles and the stator coils are hollow structure, the magnetic field in the motor is unsaturated. The whole torque can be calculated by the torque of single PM pole and a coil in superposition principle [30], [31]. This paper uses the virtual displacement method to analyse the electromagnetic torque between a single stator coil and 40 permanent magnets. When a small displacement occurs between the stator winding and the rotor poles, according to the law of conservation of energy, the energy input power change  $\Delta W_e$  of the system is equal to mechanical energy Sum of change  $\Delta W_m$  and magnetic energy storage change  $\Delta W_f$ .

The magnetic energy  $\Delta W_m$  in a magnetic field can be expressed as:

$$\Delta W_e = \Delta W_m + \Delta W_f \quad (1)$$

According to the hypothesis:  $\Delta W_e$  then:

$$\Delta W_f = -\Delta W_m \quad (2)$$

When the motor rotates at a small angle  $\Delta\theta$ , we can get:

$$T = \frac{-\Delta W_m}{\Delta\theta} \quad (3)$$

The energy of magnetic field in the whole solution domain system is:

$$\Delta W_m = \iiint \left( \int_0^B H dB \right) dv \quad (4)$$

A model of a single pair of permanent magnets and coils is established in Ansoft Maxwell software, and the electromagnetic torque is obtained by the virtual displacement method. Through the software simulation analysis, we can see that in the model of single pair of permanent magnet and coil, the electromagnetic torque will change with the change of angle. From  $0^\circ$  to the beginning, the electromagnetic torque will increase rapidly. When the deflection is about  $8^\circ$ , the torque will reach the maximum value, and then the torque will decrease slowly to 0 when the reduction is about  $30^\circ$ . That is to say, between  $0^\circ$  and  $30^\circ$ , the electromagnetic torque first rises to the maximum value and then gradually falls to  $0^\circ$  at  $30^\circ$ , which is a changing process. Based on this, the relationship between the torque and angle of single pair of permanent magnet and coil is analysed, and then the torque of the whole motor is further analysed.

In order to calculate the overall torque of PMSM, Combined with simulation analysis result, the approximate fitting function of a single permanent magnet pole and a single coil can be obtained by polynomial fitting method, and its form is as follows:

$$f(\theta_{ab}) = \sum_{n=0}^8 p_n \theta_{ab}^n \quad (5)$$

Where,  $n$  is the degree of the fitted polynomial and  $p_n$  is the coefficient of the fitted polynomial:

$$p_8 = -3.7513e - 007, p_7 = 3.5935e - 006;$$

$$p_6 = -1.2886e - 005, p_5 = 7.2226e - 005;$$

$$p_4 = -8.9598e - 005, p_3 = -1.4238e - 004;$$

$$p_2 = 3.2956e - 004, p_1 = 0.0191;$$

$$p_0 = 4.2857e - 004.$$

The whole torque can be got

$$T = \sum_{a=1}^{24} \sum_{b=1}^{40} f(\theta_{ab}) \frac{s_a \times s_b}{|s_a \times s_b|} N I_a \quad (6)$$

Where  $f(\theta_{ab})$  is the torque of one PM pole and one coil.  $s_a, s_b$  are the position vector of the PM poles and coils respectively.  $I_a$  is the current of the coils,  $N$  is the turns of the coils. The torque of one coil when rotor rotates around the Z axis and Y axis on the rotor can be divided to three components  $T_x, T_y$ , and  $T_z$ . The torque is computed in superposition principle and the FEA method respectively to test the accuracy of the superposition principle.  $\beta, \gamma$  is the angle that the rotor rotates around Y axis and Z axis, respectively.

In order to calculate the electromagnetic torque and to show the torque distribution in X-axis direction

between the two methods, the results are shown in Figures 2 and 3.

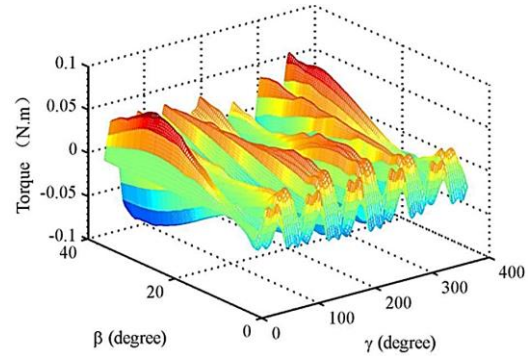


Figure 2. The relationship between X-axis rotation moment and rotation angle in superposition principle

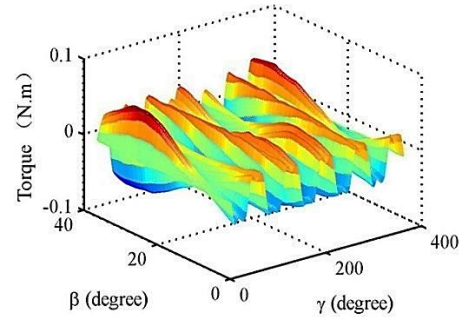


Figure 3. The relationship between X-axis rotation moment and rotation angle in FEA method

From the comparative analysis of the results in Figure 2 and Figure 3, it can be seen that the finite element modelling used to obtain the electromagnetic torque of a single permanent magnet pole and a single coil has high accuracy.

When using the superposition principle, the magnetic field saturation inside the spherical motor is ignored, so that the electromagnetic torque value is slightly larger than the torque value in the FEA method, but the error between the two is within a reasonable range.

It can be seen that using the superposition principle to obtain the correctness of the overall torque, it is only necessary to calculate the torque of a single pair of permanent magnet poles and stator coils, and then superimpose.

### 3. PSO-BP electromagnetic torque modelling

The neural network can simulate the neuron transmission process in the human brain, continuously learning external knowledge, and saving the learned knowledge in the neuron. Neural network with the advantages of good fault tolerance, strong classification ability, parallel processing ability and self-learning ability has a wide application in building regression modelling and speech recognition. As research continues to deepen, there are more optimized neural network algorithms. For example, the recurrent neural network (RNN), the long short term memory (LSTM) neural network and PSO-BP neural network are

developed to build a more accurate calculation modelling. Among them, the PSO-BP neural network obtains wide application. Here the method is applied to analyse the relationship between the structure parameters of the PMSM and the torque. In other words, PSO-BP neural network is used to model the structure and torque of the motor, so as to accurately predict the relationship between the structure and torque, which makes preparation for the next-step optimization. Moreover, simulation experiments examine modelling accuracy by comparing BP neural network regression algorithm.

### 3.1 FEA to obtain modelling data

The FEA method has high calculation accuracy and has been widely used in industry. The modelling of single PM pole and a coil is established in Ansoft Maxwell software. And the initial parameters of FEA modelling are shown in the basic structure of PMSM. When the structural parameters change, the relationship between the structural parameters and the torque of the PMSM under the new structural parameters is obtained by using FEA method again and again, enough sample data is obtained. Finally, the neural network is used to complete the modelling. the value ranges of the variable factors and the incremental step for these structural parameters are shown in Table 1.

**Table 1.** Variable levels

Factor	Level1	Level2	Level3	Level4	Level5
$r_1$ (mm)	56	58	60	62	64
$h_1$ (mm)	8	10	12	/	/
$r_2$ (mm)	6	8	10	/	/
$NI$	800	1600	2400	3200	/
$r_3$ (mm)	4	6	8	/	/
$r_4$ (mm)	14	16	18	/	/
$h_2$ (mm)	23	25	27	/	/

Because there are many parameter variables of the motor, this article chooses the experimental method of factorial design to design the structural parameters of the motor. There are  $5 \times 3 \times 3 \times 3 \times 3 \times 3 \times 4 = 4860$  combinations in factorial design totally. 4560 sample data were selected as training data and 300 sample data as prediction data.

### 3.2 PSO-BP regression modelling

BP neural network is a kind of multilayer feed-forward neural network. The main characteristics of this network are forward signal transmission and backward propagation of errors. In forward transfer, the input signal is processed layer by layer from the input layer through the hidden layer to the output layer. The neuron status of each layer only affects the neuron status of the next layer. If the output layer does not get the desired output, it switches to back propagation and adjusts the network weights and thresholds according to the prediction error, so that the predicted output of the BP neural network is constantly approaching the expected output. In this paper, PSO algorithm and BP neural network algorithm are combined to build a more accurate structure torque prediction model. PSO-BP uses the particle swarm optimization algorithm to

correct the weights  $w$  and thresholds  $b$  of the BP neural network, which can further improve the accuracy of modelling. The optimization step is divided into five steps.

The first step is to initialize particle weights  $w$  and thresholds  $b$ .

The second step is to calculate the fitness function of particles.

The third step is to update the speed and position of the particles.

The fourth step is to update the particle optimal value and the group optimal value.

The fifth step is to determine whether the maximum number of iterations has been reached. If it is: output the optimized weights  $w$  and thresholds  $b$ , the program ends. If not: return to the third step and continue to execute the relevant steps.

The following describes the calculation principle and steps of BP neural network. When arbitrary distinct training samples are given, the PSO-BP neural network with hidden nodes and activation function can be expressed as:

$$H_j = g(\sum_{i=1}^n w_{ij} x_i - b_j) \quad j = 1, 2, \dots, l \quad (7)$$

where:  $l$  is the number of the hidden layer;  $n$  is the training samples;  $w_{ij}$  is the weights connected the input layer and the hidden layer;  $b_j$  is the thresholds of the hidden layer;  $H_j$  is the output of the hidden layer;  $g(x)$  is the activation function of the hidden layer.

The output of the network  $O_k$  can be expressed as:

$$O_k = u(\sum_{j=1}^l H_j w_{jk} - b_k) \quad k = 1, 2, \dots, m \quad (8)$$

where:  $u(x)$  is the relationship between hidden layer and output layer;  $m$  is the number of the output;  $w_{jk}$  is the weights connected the hidden layer and output layer;  $b_k$  is the thresholds of the output layer.

### 3.3 Simulation analysis

When the prediction modelling is completed, the accuracy of modelling should be considered. To test the model accuracy, the mean absolute error  $MAE$  and mean absolute percentage error  $MAPE$  are selected as the measurement index, which can represent the regression ability. The definition of them can be expressed as follows:

$$MAE = \frac{1}{N} \sum_{i=1}^N |y_i - O_i| \quad (9)$$

$$MAPE = \frac{1}{N} \sum_{i=1}^N \frac{|y_i - O_i|}{y_i} \times 100\% \quad (10)$$

where  $y_i$  is the FEA test data, and  $O_i$  is the forecast data of the model.

The number of the training sample  $N$  is 4560, the number of neurons in the hidden layers  $l$  is 20 and the number of hidden layers  $q$  is 1. After calculation, the calculated  $MAE$  values of BP and PSO-BP are 0.0130 and 0.0022, respectively. And the calculated  $MAPE$  values of BP and PSO-BP are 5.36 % and 1.00 %, respectively.

This paper selects 100 sampling points and compares the actual test data with the prediction data of BP neural network algorithm and PSO-BP neural network algorithm. It can be clearly seen that the accuracy of

PSO-BP neural network modelling is higher than that of BP neural network without PSO algorithm optimization and closer to the test value.

The simulation results are shown in Figure 4.

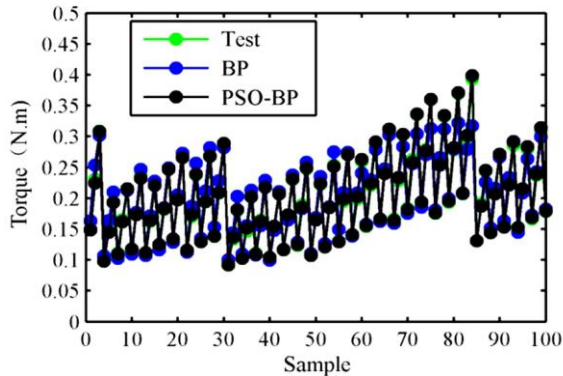


Figure 4. Accuracy comparison result

It can be seen from Figure 4 that the trend between the predicted data value and the measured value of the BP neural network is the same. The value of *MAE* and *MAPE* is closed to 0, which indicates the regression modelling has high accuracy. The simulation results shown in Figure 4 indicate the PSO-BP is more accurate than the BP neural network, which makes a better preparation for the next-step optimization.

#### 4. Multi-objective design optimization of PMSM in AGA-MOPSO

Particle Swarm Optimization (PSO) was first proposed by Eberhart and Kennedy in 1995. Its basic concept originates from the research of bird swarm foraging behaviour. Imagine a scenario in which a group of birds are searching for food randomly, and there is only one piece of food in this area. All the birds do not know where the food is, but they know how far the current position is from the food. The PSO algorithm is inspired from this behaviour of biological populations and used to solve optimization problems. A particle is used to simulate the above-mentioned bird individual. Each particle can be regarded as a search individual in the N-dimensional search space. The current position of the particle is a candidate solution corresponding to the optimization problem. The particle's flight process is the individual Search process. The particle's flying speed can be dynamically adjusted according to the historical optimal position of the particles and the historical optimal position of the population. Particles have only two attributes: speed and position, where speed represents the speed of movement and position represents the direction of movement. The optimal solution that each particle searches individually is called the individual extreme value, and the optimal individual extreme value in the particle swarm is the current global optimal solution. Keep iterating, updating speed and position.

Finally, the optimal solution that satisfies the termination condition is obtained. AGA-MOPSO builds the adaptive grid to calculate the density of the particles, based on the information of density, delete

the particle with bigger density to ensure the diversity and distribution of the solutions.

#### 4.1 Multi-objective optimization problems

Objective optimization problem generally means to obtain the optimal solution of objective function through certain optimization algorithm. When the objective function of optimization is one, it is called single objective optimization problem (SOP). When there are two or more objective functions, it is called multi-objective optimization problem (MOP). The solution of multi-objective optimization is usually a group of equilibrium solutions. There are two kinds of multi-objective optimization algorithms: traditional optimization algorithm and intelligent optimization algorithm. The traditional optimization algorithms include weighted method, constrained method and linear programming method. In essence, they transform multi-objective function into single objective function, and solve multi-objective function by using single objective optimization method. Intelligent optimization algorithm includes evolutionary algorithm (EA) and particle swarm optimization (PSO).

In this paper, optimization involves two objectives. One is the torque of the PMSM  $f_1$ , the other is the volume of the effective material  $f_2$ . The objective function of the optimal design problem for torque and volume of the effective material is as follows:

$$\begin{cases} \max f_1 = O(r_1, r_2, h_1, r_3, r_4, h_2, NI) \\ \min f_2 = \pi * r_2^2 * h_1 + \pi * (r_4^2 - r_3^2) * h_2 \end{cases} \quad (11)$$

The relationship between cross-section area of stator coil and ampere-turn number  $NI$  can be expressed as :

$$(r_4 - r_3) * h_2 = \frac{NI}{8.64} \quad (12)$$

Therefore, the constraints for multi-objective optimization problems can be expressed as :

$$\begin{cases} 56 \leq r_1 \leq 65 \\ 6 \leq r_2 \leq 12 \\ 8 \leq h_1 \leq 12 \\ 4 \leq r_3 \leq 8 \\ 14 \leq r_4 \leq 18 \\ 23 \leq h_2 \leq 27 \\ 800 \leq NI \leq 3200 \\ r_4 > r_3 \\ (r_4 - r_3) \cdot h_2 = \frac{NI}{8.64} \\ r_2 < \frac{(r_1 - h_1) * \sqrt{2} * \pi}{20} \end{cases} \quad (13)$$

Formula (13) shows the mathematical constraints among the structural parameters of the spherical motor. It provides the basis for optimizing the minimum volume target.

#### 4.2 AGA-MOPSO algorithm

AGA-MOPSO algorithm, as a fast and accurate optimization algorithm, is widely used in actual production and life. The algorithm principle and specific steps will be introduced here. In view of the disadvantages of the existing multi-objective evolutionary algorithm, such as high computational

complexity and low search efficiency, AGA-MOPSO algorithm based on adaptive grid is used. Its features include three parts.

The first part is that adaptive grid algorithm to evaluate the particle density estimation information in non-inferior solution set.

The second part is that Pareto optimal solution search technology based on AGA which can balance the global and local search capabilities.

The third part is that deleting non inferior solution in order to maintain the non-inferior solution set in a certain scale, the cut-off technology based on AGA for the non-inferior solution set is proposed.

AGA-MOPSO algorithm has good performance in solving complex large-scale optimization problems.

The steps of the optimization design divide into five steps:

**Step 1:** Initialize the maximum number of iterations  $MaxIt$ , the number of the particles  $nPop$  every iteration, the number of the particles  $nrep$  in Pareto frontier surface, inertia weight  $w$ , individual learning factor  $c_1$ , group learning factor  $c_2$ .

**Step 2:** Initialize the position and velocity of the particles. Obtain the torque  $f_1$  of the particles in PSO-BP neural network, compute the fitness  $\frac{1}{f_1}$  and the other fitness  $f_2$  every particle, get the Pareto-optimal solutions and preserve them. Build the grid. M-dimensional target space is divided into  $k_1 \times k_2 \times k_3 \times \dots \times k_m$  units, the length each grid can be calculated as

$$d_i = \frac{\max f_i(x) - \min f_i(x)}{k_i} \quad (x \in X) \quad (14)$$

where  $i$  is the  $i$ th objective,  $d$ ,  $X$ ,  $k$ ,  $f(x)$  denote the length of grid, the group of the particles, the number of the grid and the value of the function respectively.

**Step 3:** Update the velocity and position of particles. Calculate the density of the particles and select the particles which the value of the density are smallest as the global optimal solution  $gbest$ , if the number is more than one, select the particle with the highest number which dominants the particles generated every generation. Compare the particle with the old particle, if the new particle dominants the old particle, select the new particle as the individual optimal solution  $pbest$  every particle, if not,  $pbest$  is still the old particle.

**Step 4:** Preserve the non-dominated solutions and update the grid and calculate the density of the particles. If the number preserved particles are over the value of  $nrep$ , then delete the particles that the density of the particle is bigger.

**Step 5:** Repeat the step (3) and step (4). When the maximum number of iterations reaches the value of  $MaxIt$ , it ends the algorithm.

#### 4.3 Optimal results analysis

Due to the conflict and incompatibility between multiple targets, one solution is the best on one target and the worst on the other. These solutions, while improving any objective function, will inevitably weaken at least one other objective function, which is called non dominated solution or Pareto solution.

The set of optimal solutions of a set of objective functions is called Pareto optimal set. The surface formed by the optimal set in space is called Pareto frontier. Through multiple iterations, the Pareto frontier surface of the multi-objective optimization is shown in Figure 5.

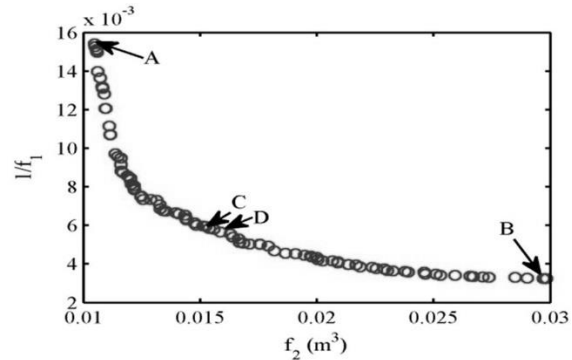


Figure 5. The Pareto fronts for the design optimization

As shown in Figure 5, the vertical axis is the reciprocal of torque  $\frac{1}{f_1}$ , the horizontal axis is the volume of the effective material  $f_2$ . In order to facilitate the analysis, the four points of A, B, C, and D are selected in the diagram we can see that the closer to point A, the better the performance of the volume of the effective material, the closer to point B, the better the performance of the torque. The specific optimization results are shown in Table 2.

Table 2. Comparison of PMSM optimization design

Factor	A	B	C	D
$r_1$ (mm)	63	65	64.98	64.28
$h_1$ (mm)	8	12	8	9.93
$r_2$ (mm)	6	10.62	10.27	10.33
$NI$	1194	3200	1509	1377
$r_3$ (mm)	8	4	6.66	8
$r_4$ (mm)	14	18	14.19	14.80
$h_2$ (mm)	23.03	26.46	23.18	23.45
Torque( $Tm$ )	0.0659	0.3174	0.1499	0.1616
Volume( $m^3$ )	0.0121	0.0299	0.0150	0.0165

The single objective optimization results are obtained further. It is easy to obtain the minimum value of  $f_2$  when  $r_1$  is 56 mm,  $h_1$  is 8 mm,  $r_2$  is 6 mm,  $NI$  is 1192,  $r_3$  is 8 mm,  $r_4$  is 14 mm,  $h_2$  is 23 mm,  $f_2$  obtains the smallest value  $0.0104 m^3$ . The maximum of torque  $f_1$  is obtained in PSO algorithm. When  $r_1$  is 63.26mm,  $h_1$  is 11.58 mm,  $r_2$  is 11.38 mm,  $NI$  is 2870,  $r_3$  is 5.64 mm,  $r_4$  is 18 mm,  $h_2$  is 26.88 mm,  $f_1$  is the biggest value  $0.3218 Tm$ . Comparing the two points A and B with the single-objective optimization results, the volume of effective material performance of the point A and the torque of the point B is slightly better than the single-objective optimization. It shows that the optimal solution set is approaching the real Pareto front better.

Finally, the optimized solution can be selected according to the need of the task.

According to the optimal parameters of point A, B, C and D, the torque generated by single PM pole and a coil of the PMSM is obtained in FEA method, as shown in Figure 6.

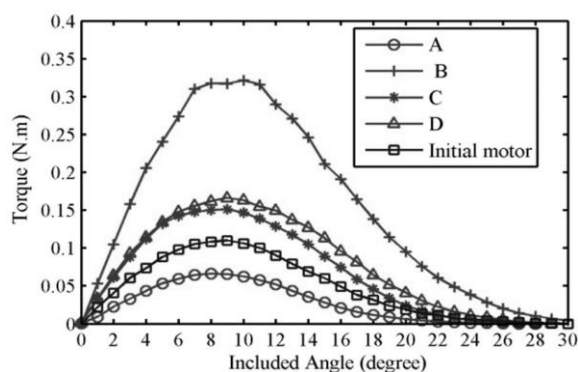


Figure 6. Comparison of initial PMSM with optimized PMSM

The volume of the effective material of the point A reduces  $0.0058 m^3$ , while the torque of point A reduces  $0.0462 Nm$ . The torque of point B increases  $0.2053 Nm$  at the cost of increased volume of the effective material. Select the point D to analyse in detail. The torque is increased from  $0.1121 Nm$  to  $0.1616 N \cdot m$ , and the volume of effective material is decreased from  $0.0179 m^3$  to  $0.0165 m^3$ . The total torque of the optimal motor can be obtained through superposition principle further.

## 5. Conclusions

An effective multi-objective design optimization method that combines PSO-BP neural network with AGA-MOPSO algorithm for the PMSM is used in this paper. Then BP neural network and PSO-BP neural network are used to map the nonlinear and complex relationship between the torque of PMSM and the structure parameters. The accuracy test in PSO-BP neural network shows that *MAE* is closed to 0.0022 and *MAPE* is closed to 1%, which is more accurate than the BP neural network. The AGA-MOPSO algorithm is proposed to optimize the structure of the PMSM. After 300 iteration optimizations of the algorithm, the Pareto-optimal solutions are obtained. Compared with the non-optimized initial model, the proposed method increases the torque by at most 181.88% and decreases the volume of the effective material by at most 48.01%. This method avoids the one-sidedness and conflict due to the optimization of exclusively one objective. It is practical than the traditional multi-objective design optimization algorithm considering the weights between different objectives. At the same time, the Pareto-optimal solutions are obtained and the designers can have many alternative solutions to choose. This method provides reference for the optimization design of other motors.

## 6. Bibliographic References

- [1] Yan, Liang, Liu, Delon, Jiao, Zongxia, Chen, Chin-Yin, Chen, I.-Ming, "Magnetic field modelling based on geometrical equivalence principle for spherical

actuator with cylindrical shaped magnet poles", *Aerospace Science and Technology*, 2016, vol. 49, no. 1, pp. 17-25, ISSN 1270-9638.

- [2] Chabt, J., Schaub, H., "Spherical magnetic dipole actuator for spacecraft attitude control", *Journal of Guidance, Control, and Dynamics*, 2016, vol. 39, no. 4, pp. 911-915, ISSN 0731-5090.
- [3] Yao Duan, Dan M. Ionel, "A review of recent developments in electrical machine design optimization methods with a permanent-magnet synchronous motor benchmark study", *IEEE Transaction on Industry Applications*, 2013, vol. 49, no. 3, pp. 1268-1275, ISSN 0093-9994.
- [4] Hu, Y., Ding, W., Wang, T., Li, S., Yang, S., "Investigation on a multi-mode switched reluctance motor: Design, optimization, electromagnetic analysis and experiment", *IEEE Transactions on Industrial Electronics*, 2017, vol. 64, no. 16, pp. 9886-9895, ISSN 1557-9948.
- [5] Wu, S., Zhao, X., Jiao, Z., Luk, C.K., Jiu, C., "Multi-objective optimal design of a toroidally wound radial-flux Halbach permanent magnet array limited angle torque motor", *IEEE Transactions on Industrial Electronics*, 2017, vol. 64, no. 4, pp. 2962-2971, ISSN 1557-9948.
- [6] Cai, Jiong-Jiong, Lu, Qinfen, Huang, Xiaoyan, Ye, Yunyue, "Thrust ripple of a permanent magnet LSM with step skewed magnets", *IEEE Transactions on Magnetics*, 2012 vol. 48, no. 11, pp. 4666-4669, ISSN 0018-9464.
- [7] Yan, Liang, Liu, Yinghuang, Jiao, Zongxia, "Electromagnetic modelling and structure optimization of a spherical force sensing system", *Sensors (Switzerland)*, 2019, vol. 19, no. 3, pp. 1-17, 2019, ISSN 1424-8220.
- [8] Liu, Chao, "Torque analysis and stator optimization of a permanent magnet spherical motor", *Tianjin University*, 2012.
- [9] Lei, G., Liu, C. C., Zhu, J. G., Guo, Y. G., "Techniques for multilevel design optimization of permanent magnet motors", *IEEE Transactions on Energy Conversion*, 2015, vol. 30, no. 4, pp. 1574-1584, ISSN 0885-8969.
- [10] Li, Z., Zhang, L., Lun, Q., Jin, H., "Optimal design of multi-DOF deflection type PM motor by response surface methodology", *Journal of Electrical Engineering & Technology*, 2015, vol. 10, no. 3, pp. 965-970, 2015, ISSN 1975-0102.
- [11] Ju, Lufeng, Wang, Qunjing, Li, Guoli, Hu, Cungang, Qian, Zhe, "Parameter optimization of support vector machine modelling for permanent magnet spherical motor", *Transactions of China Electrotechnical Society*, 2014, vol. 29, no. 1, pp. 85-90, ISSN 1000-6753.
- [12] Ju, Lufeng, Qian, Zhe, Li, Guoli, Zhou, Rui, "Research on torque optimization of the spherical motor based on SVM", 2016 IEEE 11th Conference on Industrial Electronics and Applications, Hefei, China, 2016, pp. 1786-1790.
- [13] Guo, Xiwen, Li, Guoli, "Performance prediction modelling for centrifugal pump based on BP neural network", *Electrotehnica, Electronica, Automatica (EEA)*, 2016, vol. 64, no. 3, pp. 91-95, ISSN 1582-5175.
- [14] Yeliz, Karaca, Carlo, Cattani, Majaz, Moonis, "Comparison of deep learning and support vector

- machine learning for subgroups of multiple sclerosis”, *Lecture Notes in Computer Science (including subseries Lecture Notes in Artificial Intelligence and Lecture Notes in Bioinformatics)*, 2017, vol. 10405, pp. 142-153, ISSN 0302-9743.
- [15] Joaquín, Abellán, Carlos J., Mantas, Javier G., Castellano, “A Random Forest approach using imprecise probabilities”, *Knowledge-Based Systems*, 2018, vol. 134, pp. 72-84, ISSN 0950-7051.
- [16] Liu, Qiaobin, Shi, Wenku, Chen, Zhiyong, “Rubber fatigue life prediction using a random forest method and nonlinear cumulative fatigue damage model”, *JOURNAL OF APPLIED POLYMER SCIENCE*, 2019, Vol. 137, no. 14, ISSN 0021-8995.
- [17] Heung-li, Suk, “An Introduction to Neural Networks and Deep Learning”, *Deep Learning for Medical Image Analysis*, 2017, pp. 3-24, ISSN 978-0-12-810408-8.
- [18] Cheng, Pengpeng; Chen, Daoling; Wang, Jianping, “Clustering of the body shape of the adult male by using principal component analysis and genetic algorithm-BP neural network”, *Methodologies and Application* Published, 2020, ISSN 1432-7643.
- [19] Wu Zhongqiang, Du Chunqi. “The Parameter Identification of PMSM Based on Improved Cuckoo Algorithm”, *Neural Processing Letters*, 2019, vol. 50, no. 3, pp. 2701-2715, ISSN 1370-4621.
- [20] Chen, Man Hua, “The study and application of improved micro-genetic algorithm based on cauchy mutation”, *Applied Mechanics and Materials*, 2014, vol. 538, pp. 508-511, ISSN 1662-7482.
- [21] Jiao, Licheng, Zhao, Jin, “A Survey on the New Generation of Deep Learning in Image Processing (Open Access)”, *IEEE Access*, 2019, vol. 7, pp. 172231-172263, ISSN 2169-3536.
- [22] Lee, Sangmin, Kim, Younghoon, Kahng, Hyungu, “Intelligent traffic control for autonomous vehicle systems based on machine learning”, *EXPERT SYSTEMS WITH APPLICATIONS*, 2020, vol. 144, p. 113074, ISSN 0957-4174.
- [23] Abderrezek, Hadjer, Ameer, Aissa, Harmas, Mohammed N, “Robust DC/DC converter controllers using PSO”, *Electrotehnica, Electronica, Automatica (EEA)*, 2017, vol. 65, no. 1, pp. 31-37, ISSN 1582-5175.
- [24] Youssef, Mouloudi, Amine, Meziane, Mohammed, Abdellah, Laoufi, Bousmaha, Bouchiba, Othmane, Harisi, “A swarm algorithm intelligent optimization PSO in power network real, west algeria 220 kv”, *Electrotehnica, Electronica, Automatica (EEA)*, 2016, vol. 64, no. 1, pp. 55-60, ISSN 1582-5175.
- [25] Hou, Chunguang, Yu, Xiao, Cao, Yundong, Lai, Changxue) Cao, Yuchen, “Prediction of synchronous closing Time of permanent magnetic actuator for vacuum circuit breaker based on PSO-BP”, *IEEE Transactions on dielectrics and Electrical Insulation*, 2017, vol. 24, no. 6, pp. 3321-3326, ISSN 1070-987.
- [26] Gu, Bo, Hu, Hejuan, Huang, Hui, Ren, Yan, “Hybrid PSO-BP neural network approach for wind power forecasting”, *International Energy Journal*, 2017, vol. 17, no. 4, pp. 211-222, ISSN 1513-718X.
- [27] Chen, Xia, Wang, Tuo, Liang, Wei, “General aircraft material demand forecast based on PSO-BP neural network”, *International Journal of Control and Automation*, 2016, vol. 9, no. 5, pp. 407-418, ISSN 2005-4297.
- [28] Yang, Jun-Jie, Zhou, Jian-Zhong, Fang, Reng-Cun, Li, Ying-Hai, Liu, Li, “The Multi-objective particle swarm optimization based on adaptive grid algorithm”, *Journal of System Simulation*, 2008, vol. 20, no. 21, pp. 5843-5847, ISSN 1004-731X.
- [29] Qian, Zhe, Wang, Qunjing, Ju, Lufeng. “Torque Modelling and Control Algorithm of a Permanent Magnetic Spherical Motor”, *Proceedings of the 2009 12th International Conference on Electrical Machines and Systems*, Tokyo, Japan. 2009, pp. 944-949.
- [30] Li, Zhen, Lie, Yamen, Xue Zengtao, Wang, Qunjing, “Calculation and analysis of electromagnetic characteristics of fluid suspension 3-DOF motor”, *Electric Machines and control*, 2017, vol. 21, no. 4, pp. 44-52, ISSN 1007-449X.
- [31] Li, Bin, Li, Zhitian, Li, Guidan, “Magnetic Field Model for Permanent Magnet Spherical Motor With Double Polyhedron Structure”, *IEEE Transactions on Magnetics*, 2017, vol. 53, no. 12, pp. 1-5, ISSN 0018-9464.

#### Funding Sources

This work was financially supported in part by the National Natural Science Foundation of China (No. 51637001, No. 51307001), the Natural Science Research Key Program of Anhui Provincial Education Ministry (KJ2017A001), the Young Core Teacher Program of Anhui University (J01005126), and the Academic and Technology Leaders Introduction Project of Anhui University (02303203(32030049)).

#### Authors' Biographies



**Xiwen Guo** was born in Anhui Province (China), on July 9, 1983.

He graduated the Anhui University of Science & Technology, College of Electrical and Information Engineering in Huainan (China), in 2005.

He received the *PhD degree* in electrical engineering from the Hefei University of Technology (China), in 2012.

He is current an Associate Professor at the Anhui University, in Hefei (China).n Huainan (China), in 2005.

His research interests concern: special motor and its control, power electronics and electric drives, intelligent control, and motor-pump modelling.

e-mail: xwguo2008@126.com



**Ronglin Zhang** was born in Anhui Province (China), on September 29, 1996.

He graduated from the Architecture University of Anhui, College of mechanical and electrical engineering in Hefei (China), in 2019.

He is currently working towards his *M.S. degree* at the School of Electrical Engineering and Automation of the Anhui University of China.

His research interests include electromagnetic analysis and structure optimization of PMSM

e-mail: zrl0929@163.com

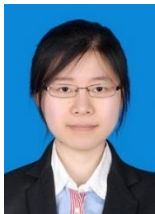


**Qunjing WANG** was born in Anhui Province (China), on July 7, 1960.

He received the *PhD* degree from University of Science and Technology of China, Hefei, China. He is currently a professor, doctoral tutor at Industrial energy saving and power quality control of collaborative innovation centre, Anhui University, in Hefei (China).

His major research interests include electrical machines, motor drives and new electric drive system.

e-mail: Wqunjing@sina.com



**Yan Wen** was born in Anhui Province (China), on April 12, 1990.

She is a *PhD* candidate in computer application technology at Anhui University, China.

Her research interests include novel spherical actuator and its control & orientation measurement, complex system modelling and analysis.

e-mail: wenyanchn@gmail.com



**Nengwei Gong** was born in Anhui Province (China), on November 12, 1994.

He graduated from the Anhui University, College of Electrical Engineering and Automation in Hefei (China), in 2017.

He is currently working towards his *M.S. degree* at the School of Electrical Engineering and Automation of the Anhui University of China.

His research interests include dynamic modelling and motion control of PMSM

e-mail: gnw1028@163.com